J Stat Phys (2011) 143: 482–500
DOI 10.1007/s10955-011-0186-y

Asymmetric Bethe-Salpeter Equation for Pairing and Condensation

Klaus Morawetz

Received: 22 December 2010 / Accepted: 17 March 2011 / Published online: 5 April 2011

Abstract The Martin-Schwinger hierarchy of correlations are reexamined and the three-particle correlations are investigated under various partial summations. Besides the known approximations of screened, ladder and maximally crossed diagrams the pair-pair correlations are considered. It is shown that the recently proposed asymmetric Bethe-Salpeter equation to avoid unphysical repeated collisions is derived as a result of the hierarchical dependencies of correlations. Exceeding the parquet approximation we show that an asymmetry appears in the selfconsistent propagators. This form is superior over the symmetric selfconsistent one since it provides the Nambu-Gorkov equations and gap equation for fermions and the Beliaev equations for bosons while from the symmetric form no gap equation results. The selfenergy diagrams which account for the subtraction of unphysical repeated collisions are derived from the pair-pair correlation in the three-particle Green's function. It is suggested to distinguish between two types of selfconsistency, the channel-dressed propagators and the completely dressed propagators, with the help of which the asymmetric expansion completes the Ward identity and is Φ-derivable.

Keywords Many-body theory · Correlations in nonequilibrium · Bethe-Salpeter equation

1 Introduction

Though pairing and condensation phenomena like superconductivity belong to the most exciting and long studied effects, their many-body theoretical treatments lacks often a systematic justifications. For example a particle-number non-conserving assumption is often

K. Morawetz (✉)
Münster University of Applied Science, Stegerwaldstrasse 39, 48565 Steinfurt, Germany
e-mail: morawetz@fh-muenster.de

K. Morawetz
International Institute of Physics (IIP), Av. Odilon Gomes de Lima 1722, 59078-400 Natal, Brazil

K. Morawetz
Max-Planck-Institute for the Physics of Complex Systems, 01187 Dresden, Germany

accepted by anomalous propagators in order to obtain the desired structure of Green's functions. Systematic many-body approximations like the ladder T-matrix [1–5] leading to the Bethe-Salpeter equation had to face the puzzle that the selfconsistent propagators describing the many-body medium have to be assumed in asymmetric form in order to obtain the gap equation. This was first observed by Kadanoff and Martin [1] and this approximation has been used mainly in the theory of superconductivity [4–6]. For an overview about different T-matrix approximations see [7]. Though any T-matrix based on the Bethe-Salpeter equation becomes unstable at the critical temperature [3] where the T-matrix diverges, the corresponding selfenergy fails to describe the superconducting gap [8] if we do not assume an asymmetry in the internal propagators.

Recently a way has been proposed to obtain such asymmetry by demanding that particles should not interact with the same state repeatedly [9]. Such non-physical repetition leads to an incorrect description of the coherent part of the scattering [10], and an incorrect single-particle Green function G. These non-physical repeated collisions destroy the superconducting gap in the energy spectrum of G. Using the Soven scheme [11] the repeated collisions can be avoided [9] and the gap in the superconducting state can be described as well as the normal state. This subtraction scheme can be written in a form equivalent to the anomalous propagator approach such that these propagators appear as consequence of the theory and need not to be assumed ad-hoc [12]. Though in this way a physical understanding of a deficiency in selfconsistent many-body expansion has already been achieved, it is desirable to see how a systematic expansion of correlations can account for such corrections.

The necessity to introduce asymmetric propagators can be seen from another physical system of dense correlated plasmas. There the motion of ions are lowered by the dynamics of the screening cloud since a deceleration force appears which is caused by the deformed screening cloud surrounding the charge. This effect known as Debye-Onsager relaxation effect has been devoted much interest [13–20] which was first derived within the theory of electrolytes [21–25]. It turned out that only an asymmetric assumption [20] about the mutual screening can correctly describe the Onsager result [16, 17, 19].

Due to the widespread usage of T-matrix approximations ranging from nuclear physics for both equilibrium [26–28] and non-equilibrium [29, 30] problems, to the theory of moderately dense gases [31] and liquid ^{3}He [32], as well as to electron-electron correlations in molecules and solids [33–37] it is desirable to clarify the correct structure of the Bethe-Salpeter equation and to specify the conditions under which the corresponding approximate forms can be used.

Here we will present a derivation of modified Bethe-Salpeter equations from first-principles which shows indeed that the hierarchical structure of correlation functions leads to such asymmetric selfconsistency as necessary to describe pairing. We will present the derivation in terms of the causal n-particle Green's functions. The cummulant expansion yields a hierarchy of correlation functions which leads already to the asymmetric result assumed by Kadanoff and Martin in binary correlation approximation.

We will then proceed and investigate the three-particle correlation and will select the processes between two pairs of particles which allow to consider the repeated collisions. We will show that the systematic cummulant expansion leads to the correct subtraction in the channels with condensates called singular channels. The idea of derivation follows here the centennial overview of many-body approximations by Heinz Puff [38] which is suited for nonequilibrium Green's function expansions. Therefore all outlined formalism holds in nonequilibrium as well as equilibrium. The expansion scheme of three-particle correlations will lead to the appearance of two different kinds of selfconsistent propagators in each considered channel. These will be the channel-dressed and the completely dressed propagators.

The outline of the paper is as follows. In the next section a scheme of Green's functions with respect to the cummulant expansion is shortly presented. This is performed with the help of the variation technique including an external potential in order to ensure the Ward-identity, ϕ-derivability and conservation laws which will be shown in the Appendix. Then we consider in the third section the binary approximation neglecting any three-particle correlation. This will lead to the Kadanoff and Martin approximation providing the correct gap equation. We discuss then the repeated collisions and how it can be avoided by a proper subtraction scheme. Though leading to the same gap equation the underlying approximation is beyond the Kadanoff-Martin form. To justify this subtraction scheme we consider in Sect. 4 the three-particle correlations. We demonstrate that the expansion of three-particle correlations in different channels leads to the distinction of two kinds of selfconsistent propagators, the channel dressed and the completely dressed one. Then we focus on the correlations between two pairs. This provides a special contribution from the pairing or condensation channel to the different channels contained in the three-particle correlations. It turned out that this selfenergy contribution provides exactly the subtracted scheme discussed in Sect. 3 and which was proposed by Lipavský [9]. In the Appendix we proof the Ward identity and the Φ-derivability in order to ensure conservation laws. We summarize and emphasize that the hierarchical dependence of correlation care for the avoidance of unphysical repeated collisions itself. As a consequence the T-matrix schemes used so far should be revised as soon as singular channels appear like in phenomena of condensation or pairing in such a way that an asymmetry in the selfconsistency is proposed.

2 Decoupling Scheme of Correlations

The n-particle causal Green's function

$$G(1,2,\ldots,n,1',2',\ldots,n';U)=\frac{1}{i^n}\frac{\langle TS\Psi_1\cdots\Psi_n\Psi_{1'}^+\cdots\Psi_{n'}^+\rangle}{\langle TS\rangle},$$
$$S=\mathrm{e}^{\int d1\Psi_1^+\Psi_1U(1)} \tag{1}$$

of a system under the influence of an external field $U(1)$, where numbers $1,2,\ldots$ sign cumulative indices like space, time, ... coordinates, can be formally represented by a generating functional

$$G(1,2,\ldots,n,1',2',\ldots.,n';U)=\partial_{\eta_{n'}}\cdots\partial_{\eta_{1'}}\partial_{\lambda_1}\cdots\partial_{\lambda_n}\mathcal{G}[\lambda,\eta]\big|_{\lambda=\eta=0} \tag{2}$$

with

$$\mathcal{G}[\lambda,\eta]=1+\sum_1^n\frac{1}{(n!)^2}\int d1\cdots dnd1'\cdots dn'\lambda_n\cdots\lambda_1G(1\cdots n';U)\eta_{1'}\cdots\eta_{n'} \tag{3}$$

where η, λ are Bose/Fermi-commuting auxiliary fields.

The Martin-Schwinger hierarchy [39] coupling the one-particle Green's function to the two-particle one,

$$\left[i\partial_{t_1}+\frac{\nabla_{r_1}^2}{2m}-U(1)\right]G(11';U)=\delta(1-1')\mp i\int d\bar{1}V(1,\bar{1})G(1\bar{1}1'\bar{1}^+;U), \tag{4}$$

is expressed in terms of this generating functional by

$$\left[i\partial_{t_1} + \frac{\nabla_{r_1}^2}{2m} - U(1)\right]\partial_{\lambda_1}\mathcal{G} = \eta_1\mathcal{G} \mp i\int d\bar{1}V(1,\bar{1})\partial_{\eta_{\bar{1}^+}}\partial_{\lambda_{\bar{1}}}\partial_{\lambda_1}\mathcal{G}. \tag{5}$$

The upper sign denotes fermions the lower bosons hereafter. It is now useful to introduce the correlated n-particle Green's function as the cummulant expansion [40] due to a new generating functional $\mathcal{G}_c$,

$$\mathcal{G}[\lambda,\eta] = \exp^{\mathcal{G}_c[\lambda,\eta]} \tag{6}$$

with

$$\mathcal{G}_c[\lambda,\eta] = \sum_1^n \frac{1}{(n!)^2}\int d1\cdots dnd1'\cdots dn'\lambda_n\cdots\lambda_1 G_c(1\cdots n';U)\eta_{1'}\cdots\eta_{n'}. \tag{7}$$

The comparison of (6), (7) and (3) with respect to the orders of λ, η reveals the cummulant expansion. The first order reads

$$G(11';U) = G_c(11';U), \tag{8}$$

i.e. the single-particle Green's function equals its correlated part. The second order shows just the separation of the Hartree-Fock term from the two-particle Green's function

$$\begin{aligned} G(121'2';U) &= G_c(121'2';U) \\ &\quad + G(11';U)G(22';U) \mp G(12';U)G(21';U). \end{aligned} \tag{9}$$

The third order is given by all possible exchanges of three one-particle Green's functions together with all possible exchanges of the two-particle correlated Green's function and a one-particle Green's function.

Introducing (6) into (5) and notating the inverse Hartree-Fock Green's function with

$$\begin{aligned} G_{\mathrm{HF}}^{-1}(12;U) &= -iV(12)G(12;U) \\ &\quad + \left[i\partial_{t_1} + \frac{\nabla_{r_1}^2}{2m} - U(1) \pm i\int d\bar{1}V(1\bar{1})G(\bar{1}\bar{1}^+;U)\right]\delta(1-2) \end{aligned} \tag{10}$$

one can invert the differential equation (5) into an integral equation

$$\partial_{\lambda_1}\mathcal{G}_c = \mathcal{I}(1) \tag{11}$$

with

$$\begin{aligned} \mathcal{I}(1) &= \int d\bar{1}G_{\mathrm{HF}}(1\bar{1};U)\eta_{\bar{1}} \mp i\int d\bar{1}d\bar{2}G_{\mathrm{HF}}(1\bar{1};U)V(\bar{1}\bar{2}) \\ &\quad \times \left\{\partial_{\eta_{\bar{2}^+}}\partial_{\lambda_{\bar{2}}}\partial_{\lambda_{\bar{1}}}\mathcal{G}_c \right. \\ &\quad + [\partial_{\eta_{\bar{2}^+}}\partial_{\lambda_{\bar{2}}}\mathcal{G}_c - G(\bar{2}\bar{2}^+;U)]\partial_{\lambda_{\bar{1}}}\mathcal{G}_c \\ &\quad \mp [\partial_{\eta_{\bar{2}^+}}\partial_{\lambda_{\bar{1}}}\mathcal{G}_c - G(\bar{1}\bar{2}^+;U)]\partial_{\lambda_{\bar{2}}}\mathcal{G}_c \\ &\quad \times \left.\partial_{\eta_{\bar{2}^+}}\mathcal{G}_c[\partial_{\lambda_{\bar{2}}}\partial_{\lambda_{\bar{1}}}\mathcal{G}_c + \partial_{\lambda_{\bar{2}}}\mathcal{G}_c\partial_{\lambda_{\bar{1}}}\mathcal{G}_c]\right\}. \end{aligned} \tag{12}$$

Using (7) we see that from the definition the correlated Green's functions can be represented by functional derivatives of (11),

$$\begin{aligned} G_c(11';U) &= \partial_{\eta_{1'}}\partial_{\lambda_1}\mathcal{G}_c|_{\lambda=\eta=0} \\ &= \partial_{\eta_{1'}}\mathcal{I}(1)|_{\lambda=\eta=0}, \\ G_c(121'2';U) &= \partial_{\eta_{2'}}\partial_{\eta_{1'}}\partial_{\lambda_1}\partial_{\lambda_2}\mathcal{G}_c|_{\lambda=\eta=0} \\ &= \mp\partial_{\eta_{2'}}\partial_{\eta_{1'}}\partial_{\lambda_2}\mathcal{I}(1)|_{\lambda=\eta=0}, \\ G_c(1231'2'3';U) &= \partial_{\eta_{3'}}\partial_{\eta_{2'}}\partial_{\eta_{1'}}\partial_{\lambda_1}\partial_{\lambda_2}\partial_{\lambda_3}\mathcal{G}_c|_{\lambda=\eta=0} \\ &= \partial_{\eta_{3'}}\partial_{\eta_{2'}}\partial_{\eta_{1'}}\partial_{\lambda_2}\partial_{\lambda_3}\mathcal{I}(1)|_{\lambda=\eta=0}, \end{aligned} \tag{13}$$

and so on. We drop the notation of the explicit dependence on the external potential U in the following. The first equation of (13) yields for the one-particle correlated Green's function

$$G_c(11') = G_{\rm HF}(11') \mp i\int d\bar{1}\bar{2}G_{\rm HF}(1\bar{1})V(\bar{1},\bar{2})G_c(\bar{1}\bar{2}1'\bar{2}^+) \tag{14}$$

and is nothing else but the Martin-Schwinger hierarchy (4) written for the correlated parts and in integral form.

The integral equation for the two-particle Green's function is more involved and reads from the second equation of (13)

$$\begin{aligned} G_c(121'2') = i\int d\bar{1}d\bar{2}G_{\rm HF}(1\bar{1})V(\bar{1}\bar{2})\,\big\{&\mp G_c(\bar{2}\bar{1}\bar{2}^+1'2') \\ &+ G(2\bar{2}^+)\big[G_c(\bar{1}\bar{2}1'2') + G(\bar{2}2')G(\bar{1}1') \mp G(\bar{2}1')G(\bar{1}2')\big] \\ &+ G_c(\bar{1}2\bar{2}^+2')G(\bar{2}1') + G_c(\bar{1}1'2\bar{2}^+)G(\bar{2}2') \\ &\mp G_c(\bar{2}2\bar{2}^+2')G(\bar{1}1') \mp G_c(\bar{2}21'\bar{2}^+)G(\bar{1}2')\big\}. \end{aligned} \tag{15}$$

This equation is graphical presented in Fig. 1 and is exact so far. Since the following algebra is somewhat involved it is easier to perform it in terms of diagrammatic presentation. Therefore we design a complete selfconsistent one-particle Green's function with a thick full arrow, the interaction with a broken line and the two-, three-, and four-particle Green's

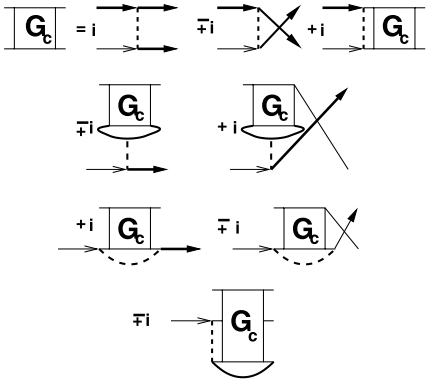

Fig. 1 The equation for the correlated two-particle Green's function. *The thin open arrows* are Hartree-Fock Green's functions, *the thick arrows* are full Green's functions. *The first line* represents the ladder approximation and *the second* and *third lines* exchange channels

functions with a square containing two, three and four legs. The Hartree-Fock Green's function is designed as thin arrow. Corresponding upper signs denote fermions and lower signs bosons. The numbering of in and outgoing channels are in the direction from bottom to top. Lines without an arrow indicates ends of two- and three particle Green's functions which are not connected with a one-particle Green's function.

From the derivation above it is not hard to see that the property

$$G_c(121'2';U) = \mp G_c(211'2';U) = \mp G_c(122'1';U) \tag{16}$$

is ensured. In other words the criterion (A) and (B) of Kadanoff and Baym is fulfilled and we have a conserving approximation, i.e. the energy, momentum and density is conserved [41]. Please note that the corresponding diagrams in the second and third line in Fig. 1 cancel each other for fermions and contact interaction, i.e. they become small for short-range interactions.

3 Two-Particle Correlations

3.1 Binary Collision Approximation

As a first very drastic approximation we want to consider the binary correlation approximation which consists in neglecting the correlated three-particle Green's function in (15), i.e. the last diagram in Fig. 1. Further we neglect also the second and third line since they vanish for fermions and short-range interaction. This results into the known ladder approximation or Bethe-Salpeter equation. Amazingly we have now obtained that the intermediate propagators of the Bethe-Salpeter equation have to be considered asymmetrically. Indeed, the vertex

$$G_c(121'2') = \int d\bar{1}d\bar{2}d\bar{1}'d\bar{2}' G_{\mathrm{HF}}(1\bar{1})G(2\bar{2})\Gamma(\bar{1}\bar{2}\bar{1}'\bar{2}')G(\bar{1}'1')G(\bar{2}'2') \tag{17}$$

can be represented in symmetrized form

$$\Gamma(121'2') = T(121'2') \mp T(122'1') \tag{18}$$

by the T-matrix

$$\begin{aligned} T(121'2') &= iV(12)\delta(1-1')\delta(2-2') \\ &\quad + i\int d\bar{1}d\bar{2}V(12)G(2\bar{2})G_{\mathrm{HF}}(1\bar{1})T(\bar{1}\bar{2}1'2'). \end{aligned} \tag{19}$$

The asymmetry appears such that a full Green function G_c is combined with a Hartree-Fock Green's function. This asymmetry is maintained if we go systematically to higher-order approximations neglecting 4-particle correlated Green's functions as we will see in the next section. It is a result of the hierarchical structure of the equations of motion. If one compares with the linearized parquet approximations [42, 43], the Hartree-Fock propagator G_{HF} in Fig. 1 is replaced by the full one G_c which includes nonphysical processes. We will see in the next section that the result derived here by the hierarchy avoids such non-physically multiple scatterings with the same channel. Therefore we consider the asymmetric form in Fig. 1 as superior to the parquet approximation.

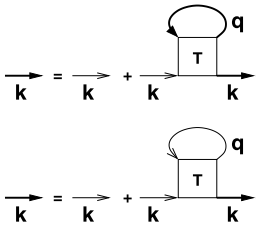

Fig. 2 The Dyson equation in ladder approximation for the symmetric selfconsistency (*above*) and the Kadanoff-Martin asymmetric one derived here (*below*)

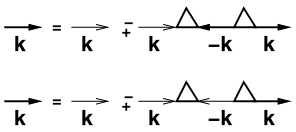

Fig. 3 The propagator equations resulting from Fig. 2, selfconsistently (*above*), Kadanoff-Martin asymmetric (*below*). The upper/lower sign stands for Fermi/Bose systems

In fact this asymmetry has been recognized as being necessary to obtain the gap equation for pairing [44]. It was first observed by Kadanoff and Martin [1] and used later on [4, 5, 9, 45] as an ad-hoc approximation seemingly violating the symmetry of equations and consequently violating conservation laws. This has remained puzzling since a worse approximation leads obviously to better results. Recently it turned out that the repeated collisions [9] with the same particle are responsible for this artifact.

3.2 Derivation of Gap Equation

Let us illustrate this by comparing the Dyson equation with symmetric and with asymmetric selfconsistency in Fig. 2. The T-matrix has poles at bound states and at the pairing and becomes separable near these poles, $T = \mp\triangle\triangle$ where the upper sign is for fermions and the lower for bosons. The two different Dyson equations for the propagator with respect to the symmetry of selfconsistency is illustrated in the next Fig. 3. The first symmetrical selfconsistent Dyson equation leads to the propagator

$$G(\omega, \mathbf{k}) = \frac{1}{\omega - \epsilon_{\mathbf{k}} \pm \Delta^2 G(-\omega, -\mathbf{k})} \tag{20}$$

which shows no pole and no gap equation. Considering the second asymmetrical Kadanoff-Martin approximation of Fig. 3 we obtain

$$G(\omega, \mathbf{k}) = \frac{1}{\omega - \epsilon_{\mathbf{k}} \mp \frac{\Delta^2}{\omega + \epsilon_{-\mathbf{k}}}} \tag{21}$$

which possesses the typical two-pole structure of the BCS gap equation in the case of fermions. Therefore the Kadanoff and Martin approximation is superior to the symmetric selfconsistent ladder approximation and appears as a consequence of the hierarchical dependencies of correlations as derived above.

What has this now to do with avoiding repeated collisions? Repeated collisions of two particles in the same state are unphysical since the particles move apart from each other after the collision. Therefore we have to ensure that due to selfconsistency such collisions with the same state do not appear. In fact as can be seen in Fig. 4, the selfconsistent Dyson equation does not ensure that the momentum of the repeated collisions, $\mathbf{p}$, is unequal to the

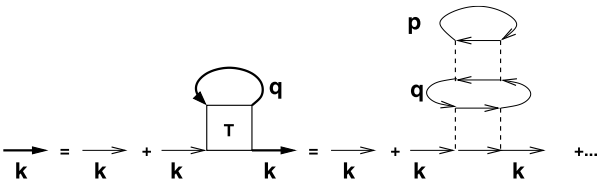

Fig. 4 The iteration of the selfconsistent Dyson equation of Fig. 2 leading to repeated collision with momentum **p**, **q**

momentum of the incoming particle **k**. If this would be the case the particle will scatter with a particle in the same state again. These repeated collisions have to be removed from the T-matrix and the correct gap equation appears and the condensate can be described without asymmetrical ad-hoc assumptions about selfconsistency. The advantage of eliminating only the contributions of single channels as proposed in [9] and [45] is that the formation of pairs and their condensation can be described within the same approximation. Explicitly, we split the selfenergy into different channels, $\Sigma = \sum_j \Sigma_j$ where we assume the condensation or pairing to appear in the channel i called the singular channel. Now we define a subtracted propagator

$$G_{\not i} = G - G_{\not i}\Sigma_i G \tag{22}$$

where the T-matrix of the channel carrying the pole, T_i, is closed by the subtracted propagator $\Sigma_i = T_i \bar{G}_{\not i}$. Writing the Dyson equation explicitly leads to the full propagator in momentum-energy representation $p = (\omega, \mathbf{p})$ [12]

$$G(p) = \frac{\omega + \epsilon + \bar{\Sigma}_{11}}{(\omega + \epsilon + \bar{\Sigma}_{11})(\omega - \epsilon - \Sigma_{11}) \mp \Sigma_{12}^2} \tag{23}$$

where $\Sigma_{11}(p) \equiv \Sigma(p) - \Sigma_i(p)$ and $\Sigma_{12}(p) \equiv \Delta(p)$ and the upper/lower sign stands for fermions/bosons. The expression (23) is nothing else but the Beliaev form for bosons [46] or the Nambu-Gorkov form for fermions [47] and can be written also in matrix notation with off-diagonal elements [12].

Though we have shown above that the Kadanoff-Martin approximation leads already to a two-pole Green's function (21) necessary for the gap equation, the alert reader has noticed that the subtraction of unphysical multiple scattering events has assumed a different intermediate propagator than the Kadanoff-Martin approximation though leading to the same gap propagator (23). The Kadanoff-Martin approximation requires to use the Hartree-Fock propagator as derived above by approximating the hierarchy of correlations at the binary level. For the subtraction of repeated collisions we have used instead the propagator written with the help of (22)

$$G_{\not i} = G_{\rm HF} + G_{\rm HF}(\Sigma - \Sigma_{\rm HF} - \Sigma_i)G_{\not i} \tag{24}$$

which shows that the subtracted propagator is beyond the Hartree-Fock one. How can we derive such a form from the hierarchy of correlations?

4 Three-Particle Approximations

4.1 Generic Structure

For this purpose we go one step further and approximate the equation for the three-particle correlation represented by the last line of (13). It shows the coupling to the four-particle

Green's function and is quite lengthy. For the sake of legibility we abbreviate the interchanges of indices of the corresponding foregoing expressions by denoting them in the following formula within the same kind of brackets,

$$
\begin{aligned}
G_c(1231'2'3') = \mp i \int d\bar{1}d\bar{2} G_{\rm HF}(1\bar{1}) V(\bar{1}\bar{2}) \big\{ & G_c(23\bar{2}\bar{1}\bar{2}^+1'2'3') \\
& \mp G_c(2\bar{2}\bar{1}1'2'3') G_c(3\bar{2}^+) \mp (2 \leftrightarrow 3) \\
& + \big\{ G_c(23\bar{2}\bar{2}^+2'3') G_c(\bar{1}1') \mp (\bar{1} \leftrightarrow \bar{2}) \\
& \mp G_c(2\bar{2}\bar{2}^+3') G_c(3\bar{1}1'2') \mp (2 \leftrightarrow 3) \\
& + [\mp G_c(3\bar{2}^+) G_c(2\bar{2}2'3') G_c(\bar{1}1') + (\bar{1} \leftrightarrow \bar{2})] \mp [(2 \leftrightarrow 3)] \\
& + G_c(23\bar{2}^+1') [G_c(\bar{2}\bar{1}2'3') + G_c(\bar{2}2') G_c(\bar{1}3') \\
& \mp G_c(\bar{2}3') G_c(\bar{1}2')] \big\} \\
& \mp \{1' \leftrightarrow 2'\} + \{1' \leftrightarrow 2' \leftrightarrow 3'\} \big\}. \qquad (25)
\end{aligned}
$$

Now we consider selected approximations by neglecting the four-particle correlation and selecting special sets of diagrams. First let us show how the known channel approximations appear which are the screened ladder, the maximally crossed diagrams and the ladder diagrams. Then we will consider the pair-pair correlations and their influence on these three channels.

4.2 Screened Ladder Approximation

We choose as partial summation from (25) the first set of diagrams indicated in Fig. 5. The diagrams obtained by interchanging $1' \leftrightarrow 2'$ and $1' \leftrightarrow 2' \leftrightarrow 3'$ in Fig. 5 are contained in (25) as well. Now the iteration of the equation for the three-particle correlated Green's function in Fig. 5 leads to a repeated sum in the interaction lines which can be summarized by introducing the screened potential of Fig. 6. This procedure results into the expression for the three-particle correlated Green's function as illustrated in Fig. 7. Introducing this expression into the last diagram of Fig. 1 one obtains the diagrams of Fig. 8. We see that the last line renormalizes the single-particle propagator if brought to the left-hand side. In such a way the equation of the two-particle Green's function in Fig. 8 can be very much

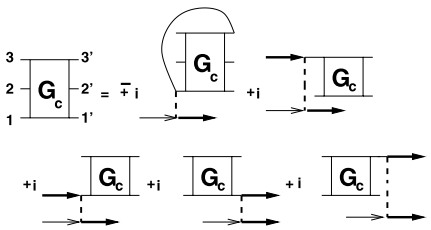

Fig. 5 A special set of diagrams for the three-particle correlated Green's function (25)

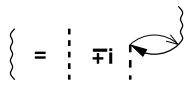

Fig. 6 Definition of the screened potential V_s

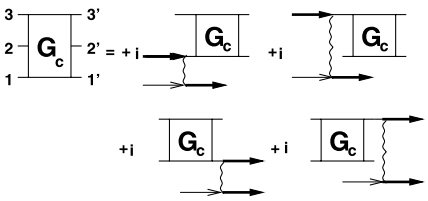

Fig. 7 The set of diagrams of Fig. 5 when introducing the screened potential of Fig. 6

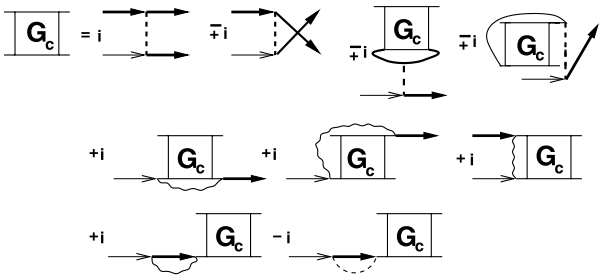

Fig. 8 The diagrams of Fig. 1 when introducing the three-particle Green's function of Fig. 7

Fig. 9 The screened propagator (26)

simplified to which end we introduce the modified propagator

$$\begin{aligned} G_s &= G_{\mathrm{HF}} + G_{\mathrm{HF}}(\Sigma_s - \Sigma_{\mathrm{F}})G_s \\ &= G_{\mathrm{H}} + G_{\mathrm{H}}(\Sigma_s)G_s \\ &= G_0 + G_0(\Sigma_s + \Sigma_{\mathrm{H}})G_s \end{aligned} \tag{26}$$

where $\Sigma_s(12) = iV_s(12)G(12)$ is the screened self energy and $\Sigma_{\mathrm{F}}(12) = iV(12)G(12)$ the Fock self energy as illustrated in Fig. 9. We will call in the following this modified propagator the channel-dressed selfconsistent propagator to distinguish him from the complete-dressed selfconsistent propagator. The channel-dressed propagator is determined by the corresponding selfenergy understood as the lowest selfconsistent diagram in the corresponding channel while the complete-dressed propagator includes all higher-order crossed terms. The introduction of this channel-dressed (screened) propagator results into the final expression of Fig. 10.

Compared to the Kadanoff-Martin approximation which was represented by diagrams of Fig. 1 neglecting the three-particle Green's function, we now obtain in Fig. 10 the same set

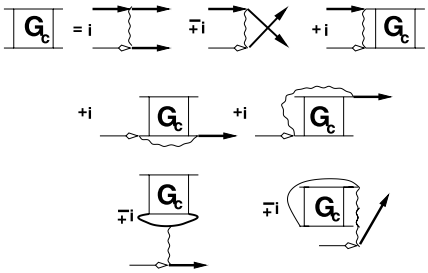

Fig. 10 The diagrams of Fig. 8 when introducing the channel-dressed propagator (26) indicated as *thin open arrows*

of diagrams except that the Hartree-Fock propagator has to be replaced by the modified one (26) and the bare interaction has to be replaced by the screened interaction of Fig. 6 in the ladders. Please note that the screened interaction appears with asymmetric propagators.

Again we see that for fermions and short range screened interaction the second and third line of diagrams in Fig. 10 are canceling mutually and only the screened ladder diagram remains. Together with the screened potential of Fig. 6 this is the screened ladder approximation used before [48] except that now one of the internal propagators has to be replaced by the screened one (26). This establishes the asymmetric form derived here as a new result.

Please note that (26) looks already like the structure of subtracting unphysical repeated collisions (24), however, only the Fock term appears to be subtracted from the screened approximation selfenergy in the propagator (26) since the scheme accounts for it already in the Bethe- Salpeter equation.

4.3 Maximally Crossed Diagrams

A next set of diagrams included in (25) is summarized by the maximally crossed ladders presented in Fig. 11 where the diagrams interchanging $1' \leftrightarrow 2'$ and $1' \leftrightarrow 2' \leftrightarrow 3'$ are contained in (25) as well. We proceed with the same steps as in the last chapter by introducing the expression of Fig. 11 into the last diagram of Fig. 1 but defining now the channel-dressed propagator

$$\begin{aligned} G_{\tilde{T}} &= G_0 + G_0 \Sigma_{\tilde{T}} G_{\tilde{T}} \\ &= G_{\rm HF} + G_{\rm HF}(\Sigma_{\tilde{T}} - \Sigma_{\rm HF}) G_T \end{aligned} \tag{27}$$

to obtain the diagrams in Fig. 12. Here the selfenergy reads

$$\Sigma_{\tilde{T}}(11') = \mp \int d\bar{1}\bar{2}\, \tilde{\Gamma}(\bar{1}1\bar{2}1') G(\bar{2}\bar{1}^+) \tag{28}$$

where the symmetrized vertex

$$\tilde{\Gamma}(1234) = \tilde{T}(1234) \mp \tilde{T}(1243) \tag{29}$$

is expressed via the maximally crossed ladders of Fig. 13.

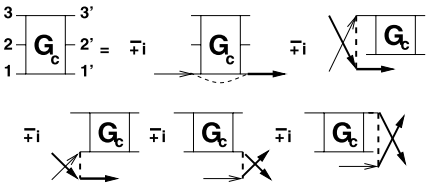

Fig. 11 The maximally crossed diagrams contained in (25)

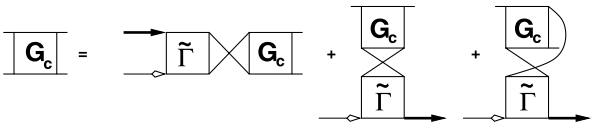

Fig. 12 The diagrams introducing Fig. 11 into Fig. 1. *The thin open arrow* mark now the channel-dressed propagator (27)

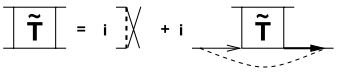

Fig. 13 The maximally crossed ladder summation

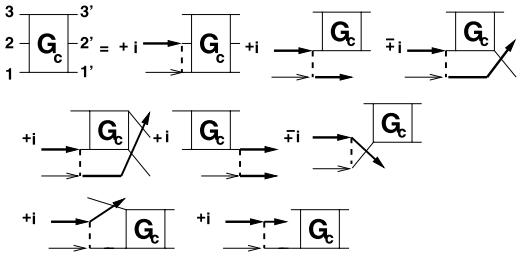

Fig. 14 The ladder diagrams contained in (25)

4.4 Ladder Diagrams

As a last set we select the ladder diagrams included in (25) which are collected in Fig. 14. Also the diagrams interchanging $2 \leftrightarrow 3$ are contained in (25).

Introducing the expression of Fig. 14 into the last diagram of Fig. 1 with the channel-dressed propagator

$$\begin{aligned} G_T &= G_0 + G_0 \Sigma_T G_T \\ &= G_{\mathrm{HF}} + G_{\mathrm{HF}} (\Sigma_T - \Sigma_{\mathrm{HF}}) G_T \end{aligned} \tag{30}$$

we obtain the diagrams in Fig. 15. Here the selfenergy reads

$$\Sigma_T(11') = \int d\bar{1}\bar{2}\, \Gamma(\bar{1}1\bar{2}1') G(\bar{2}\bar{1}^+) \tag{31}$$

and the symmetrized vertex Γ was given by (18) in terms of the ladder T-matrix (19) presented in Fig. 16.

4.5 Pair-Pair Correlation

Now that we have seen how the standard channels appear from the cummulant expansion of correlations in terms of Green's functions with special emphasis on the asymmetric propagators we proceed and investigate the pair-pair correlation. In fact in (25) there are diagrams included which describe the interaction of two two-particle Green's functions outlined in Fig. 17.

From these diagrams we search only the ones which yield a renormalization of the left-lower Hartree-Fock propagator after iteration in one of the above three channels, i.e. the

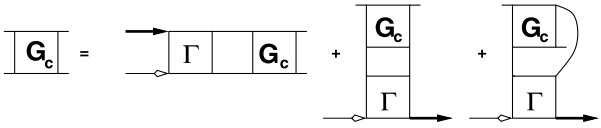

Fig. 15 The diagrams introducing Fig. 14 into Fig. 1. *The thin open arrow* are the channel-dressed propagator (30)

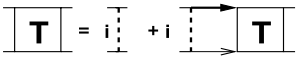

Fig. 16 The ladder summation

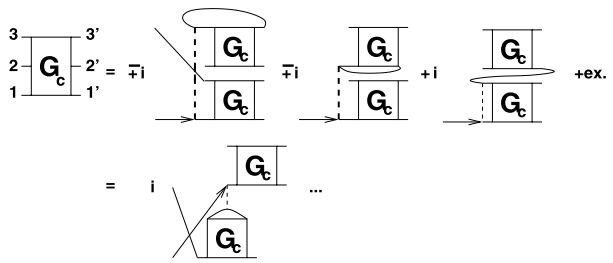

Fig. 17 The pair-pair diagrams in (25)

first responsible diagram of Figs. 5, 11 or 14 respectively. In such a way we can define a channel-dressed propagator as done repeatedly above. It turns out that only the one diagram written in the second line of Fig. 17 fulfills this task. All other diagrams give repeated iterations partially included in the above summations and partially leading to new cross diagrams. These diagrams we will not consider here. They have been partially considered in Born approximation named as cluster Hartree-Fock diagrams [49] and have been applied to exciton problems [50] and to the first-order superfluid phase transition [51]. These diagrams describe the interaction between the cluster and the single particle, while we concentrate here on a genuine cluster-cluster diagram.

We introduce now this single renormalizing diagram of the last line in Fig. 17 into the corresponding three-particle ones on the right hand sides of Figs. 5, 11 or 14. This leads to iterations which sum the interactions and result into the channel effective blocks, screened potential, maximally crossed vertex or T-matrix vertex. These diagrams are then again introduced into the last diagram of Fig. 1 as done repeatedly before. In this way we obtain an additional renormalization diagram for the channel-dressed propagators of (26), (27) and (30) which can be written

$$G_\Delta = G_p - G_p \Sigma_\Delta G_\Delta \tag{32}$$

with $p = s, \tilde{T}, T$ denoting the channels. The corresponding selfenergy Σ_Δ due to the pair-pair interaction is shown in Fig. 18 where the kernel K denotes the considered channels $V_s - V$, $i\tilde{T}$ and $iT + V$ correspondingly.

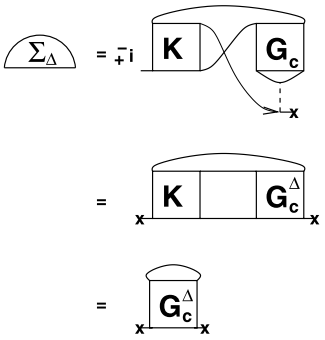

Fig. 18 The selfenergy of the renormalized propagator due to pair-pair correlations in Fig. 17 where the kernel K signs $V_s - V$ for the screened channel of Fig. 10, $i\tilde{T}$ for the maximally crossed channel in Fig. 12 and $iT + V$ for the ladder diagrams in Fig. 15. *The second line* is valid only for separable two-particle correlations, see Fig. 19, when using the screened diagrams of Fig. 8. *The third line* appears using the ladder diagrams of Fig. 15. *Crosses* denotes the inverse (amputated) propagator

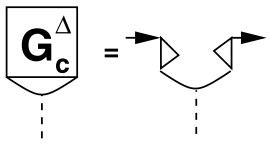

Fig. 19 Separation in in- and outgoing channels in the pole of pairing or condensation

We want to consider specially the particle-particle channel represented by the T-matrix since in this channel the pairing appears. There we have

$$\begin{aligned} G_\Delta &= G_{\rm HF} + G_{\rm HF}(\Sigma_T - \Sigma_\Delta - \Sigma_{\rm HF})G_\Delta \\ &= G_0 + G_0(\Sigma_T - \Sigma_\Delta)G_\Delta . \end{aligned} \tag{33}$$

For the singular channel, where the pairing appears, we will see now that the desired specific contribution remains. For this purpose we use the fact that the two-particle correlation separates near the pairing or condensation pole, illustrated in Fig. 19 and as it was used above in Sect. 3.2. Taking this into account we see from the screened ladder diagrams in Fig. 8 that besides the Hartree and Fock terms which appear to be subtracted in Fig. 18, only the third term in Fig. 8 remains as a connected diagram. Therefore we can replace the corresponding form in the second part of Fig. 18 by a full two-particle propagator which results into the second line of Fig. 18. Using the iteration of the T-matrix channel of Fig. 15 once more, we obtain the third line in Fig. 18. Due to this procedure we obtain the result

$$\Sigma_\Delta = \Sigma_{\not\iota} \tag{34}$$

and comparing (24) with (33) we concluded that $G_\Delta = G_{\not\iota}$. This is exactly the subtracted propagator (24) proposed before which corrects for the repeated collisions with the same state. The derived selfenergy diagram in the first line of Fig. 18 is therefore one of the main results of this paper since it presents the diagrammatic part which leads to the subtraction of unphysical repeated collisions in any channel. For the particle-particle channel we have obtained the correct subtracted propagator and see that a proper collection of pair-pair correlations in the hierarchical expansion of correlations cares for the subtraction of such unphysical processes.

5 Summary and Outlook

We have re-examined the Martin-Schwinger hierarchical structure of correlations. The expansion scheme of Green's functions has been written with the focus on the cummulant expansion form. We have investigated the binary collision approximation as well as three-particle correlations and have derived the corresponding Bethe-Salpeter equations. It appears that the two internal propagators of the resulting Bethe-Salpeter equations are asymmetric with respect to self-consistency. Dependent on the considered channel we obtain one complete-selfconsistent and one channel-dressed selfconsistent propagator. The binary collision approximation leads to one Hartree-Fock and one selfconsistent propagator in agreement with the Kadanoff and Martin form. This leads to the gap equation of pairing while the standard Bethe-Salpeter equation with two selfconsistent propagators does not.

We have proceeded to understand this asymmetry as a subtraction of repeated collision with the same state which is unphysical. Such single-channel corrections contribute to diagrammatic sums with a weight of the inverse volume and appears therefore only if one has

a singular channel carrying a condensation with a macroscopic number of occupation. It is shown that such a subtraction scheme appears if we consider the correlations of two pairs of particles contained in the three-particle correlated Green's function. We identify the self-energy diagram which is responsible for such proper subtraction scheme and show that the recently proposed scheme following the idea of Soven has its justification in the hierarchical dependence of correlations.

The here derived selfenergy correction responsible for this subtraction scheme is valid in all three considered channels, the screened ladder, the maximally crossed diagrams and the T-matrix channel. Though we had searched only for the correction of the latter one in order to obtain pairing and the gap equation we suggest that this selfenergy diagram might have an effect also to the maximally crossed diagrams. In that channel one describes weak localization phenomena. Since it was shown recently [43] that the parquet diagrammatic summation leads not to the expected Anderson localization, we suggest that the asymmetric parquet summation which appears due to the here derived selfenergy correction might solve these problems with localization. This investigation is deserved for further work.

Acknowledgements The discussions with Pavel Lipavský, Bretislav Šopík, Michael Männel and Alvaro Ferraz are gratefully mentioned. This work was supported by DFG-CNPq project 444BRA-113/57/0-1 and the DAAD-PPP program (BMBF). The financial support by the Brazilian Ministry of Science and Technology is acknowledged.

Appendix: Variational Technique, Ward Identities and Φ-Derivability

Due to the coupling of an external potential $U(11') = \delta_{11'}U(1)$ one expresses the two-particle causal Green function $G(121'2') = 1/i^2\langle T\Psi_1\Psi_2\Psi_2^+\Psi_1^+\rangle$ by a variation of the one-particle Green's function $G(12) = 1/i\langle T\Psi_1\Psi_2^+\rangle$ with respect to the external potential [52, 53] as

$$G(121'2') = G(11')G(22') \mp \frac{\delta G(11')}{\delta U(2'2)} \tag{35}$$

where the upper sign denotes the Fermi and the lower the Bose functions. Using the Dyson equation

$$G^{-1} = G_0^{-1} - \Sigma - U \tag{36}$$

one can calculated the derivative in (35) and with the help of the chain rule and $\delta G = -G\delta G^{-1}G$, the fluctuation function reads

$$\begin{aligned} L(121'2') &= G_c(121'2') + G(12')G(21') \\ &= G(121'2') - G(11')G(22') \\ &= \mp G(12')G(21') \mp G(13)\frac{\delta\Sigma(34)}{\delta U(2'2)}G(41') \\ &= \mp G(12')G(21') + G(13)\frac{\delta\Sigma(34)}{\delta G(56)}L(5262')G(41'). \end{aligned} \tag{37}$$

Double occurring indices are understood as integrated over. Equation (37) is expressed graphically in Fig. 20.

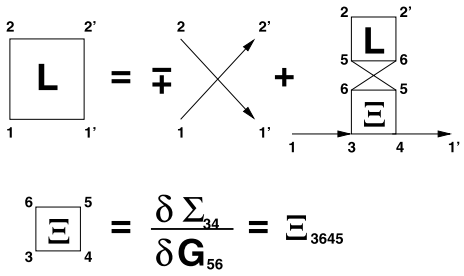

Fig. 20 Variational representation of the two-particle correlation function (37)

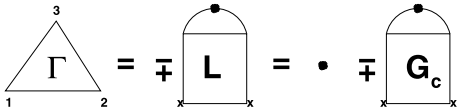

Fig. 21 Definition of the vertex function (38)

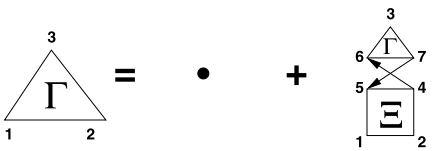

Fig. 22 Equation for the vertex function

Defining a three-point vertex function

$$\Gamma(123) = \delta_{12}\delta_{13} + \frac{\delta\Sigma(12)}{\delta U(33)}$$
$$= \delta_{12}\delta_{13} + \frac{\delta\Sigma(12)}{\delta G(45)} G(46)\Gamma(673)G(75) \tag{38}$$

illustrated in Fig. 21 the two-particle correlation function of Fig. 20 can be represented by Fig. 22.

The first line of (38) establishes the Ward identity [54–56] which is therefore a consequence of the variational expression (35) and the form of Dyson (36). This Ward identity is also a consequence of the fact that the selfenergy can be represented as variation of a Φ-functional with respect to the propagator [39]. Recently it has been proposed [57] to expand the variational scheme in terms of the kernel represented in the last line of Fig. 20.

How does this scheme fit now the asymmetric form presented in this paper? We demonstrate this on the example of the screened ladder approximation of Fig. 10. The other channels can be treated analogously. Closing the upper lines of the mirrored diagrams of Fig. 10 with the channel-corrected propagator we obtain the same form of the three-point vertex in Fig. 22 but now translated into Fig. 23 with asymmetric propagators. The kernel takes the form represented by Fig. 24 which can be verified by expanding the diagrams with the help of G_c of Fig. 10. In comparison with Fig. 22 the intermediate propagators are asymmetric.

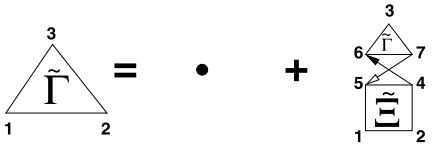

Fig. 23 Equation for the vertex function in asymmetric form

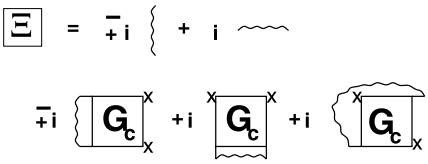

Fig. 24 Kernel of the vertex function in Fig. 22 for screened ladder channel of Fig. 10

Using the Dyson equation for the channel-dressed propagator with channel index i we can replace in one propagator of Fig. 22

$$G = G_i + G_i \Sigma_i G \tag{39}$$

and then have to show that

$$\Xi(1234) + \Xi(1235) G_i(56) \Sigma_i(64) \equiv \tilde{\Xi}(1234) \tag{40}$$

in order to proof $\tilde{\Gamma} = \Gamma$. To complete (40) we use $1 + G\Sigma_i = G G_i^{-1}$ and write

$$\begin{aligned} \tilde{\Xi}(1234) &= \Xi(1235) G_i(56) G_i^{-1}(64) \\ &\equiv \frac{\delta \Sigma(12)}{\delta \mathcal{G}(43)} = \frac{\delta \Sigma(12)}{\delta G(56)} \frac{\delta G(56)}{\delta \mathcal{G}(43)} \end{aligned} \tag{41}$$

where we have introduced the (variational) selfconsistent propagator $\mathcal{G}$ to be defined by

$$\frac{\delta G(56)}{\delta \mathcal{G}(43)} G_i(42) G(61) \equiv G(31) G(52) \tag{42}$$

illustrated in Fig. 25.

With the help of this variational propagator we can fulfill the relation (41) such that we have

$$\tilde{\Xi}(1234) = \frac{\delta \Sigma(12)}{\delta \mathcal{G}(43)}. \tag{43}$$

This, however, has the required form of Fig. 20 such that (37) is fulfilled and the Ward identities are completed. Please note that neither G nor G_i serve as propagators to perform the variation but the variational propagator $\mathcal{G}$ defined by (42).

Therefore the screened ladder approximation (and the other 2 considered channels as well) can be recast into a form of three-point vertex function which obeys an integral equation with has the desired form of Ward identity. The difference to the traditional treatment is that a full dressed propagator is combined with the channel-dressed propagator. The price we pay is that we do have two different selfconsistent propagators the channel-dressed one and the complete dressed one.

Now we can write down the standard Φ-functionals for T-matrix, screened ladder and maximally crossed channels but with symmetrical $\mathcal{G}$ propagators.

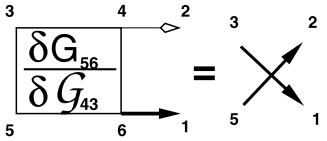

Fig. 25 Definition of the variational propagator $\mathcal{G}$ (42)

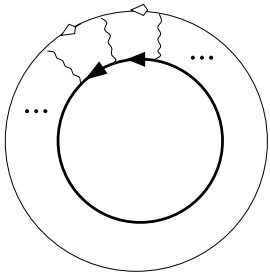

Fig. 26 The Φ-functional defining the asymmetric screened channel approximation

Alternatively we can use (42) to replace them by the two different selfconsistent propagators. Consequently, the appearance of two different propagators does not violate the Φ-derivability and the conservation laws. This can be considered alternatively by translating the known conserving approximations into forms of two different species in the system and interpret in the end one specie as the complete-dressed selfconsistent and the other specie as the channel-dressed selfconsistent propagator. For the screened ladder channel we declare e.g. a Φ-functional as illustrated in Fig. 26.

At the end it has to be remarked that the here proven Ward identity and Φ-derivability is in a sense a triviality as long as the scheme is kept exact. Any formal expansion is 'exact' and will obbey therefore these exact identities. The difference between different expansion schemes lays in the different kind of approximations 'naturally' offered. Therefore at any stage of approximation actually used, one has to ensure the Ward identity. The introduction of the variational propagator (42) in Fig. 25 shows that any asymmetric approximation proposed with the scheme in this paper can be translated into a symmetric one. However the relation is very cumbersome in such a way that any asymmetric form chosen translates into many higher order diagrams in the symmetric writing.

References

1. Kadanoff, L.P., Martin, P.C.: Phys. Rev. **124**(3), 670 (1961)
2. Bishop, R.F., Strayer, M.R., Irvine, J.M.: Phys. Rev. A **10**(6), 2423 (1974)
3. Bishop, R.F., Strayer, M.R., Irvine, J.M.: J. Low Temp. Phys. **20**(5–6), 573 (1975)
4. Maly, J., Jankó, B., Levin, K.: Phys. Rev. B **59**(2), 1354 (1999)
5. He, Y., Chien, C.C., Chen, Q., Levin, K.: Phys. Rev. B **76**(22), 224516 (2007)
6. Chien, C.C., He, Y., Chen, Q., Levin, K.: Phys. Rev. A **77**(1), 011601 (2008)
7. Chen, Q., Stajic, J., Tan, S., Levin, K.: Phys. Rep. **412**, 1 (2005)
8. Wild, W.: Z. Phys. **158**(3), 322 (1960)
9. Lipavský, P.: Phys. Rev. B **78**, 214506 (2008)
10. Watson, K.M.: Phys. Rev. **89**, 575 (1953)
11. Soven, P.: Phys. Rev. **156**(3), 809 (1967)
12. Morawetz, K.: Phys. Rev. B **81**, 092501 (2010)
13. Kadomtsev, B.B.: Pis'ma Zh. Eksp. Teor. Fiz. **33**, 151 (1958). Sov. Phys. JETP **33**, 117 (1958)
14. Klimontovich, Y.L., Ebeling, W.: Pis'ma Zh. Eksp. Teor. Fiz. **63**(3(9)), 904 (1972)
15. Ebeling, W.: Ann. Phys. **33**, 5 (1976)
16. Ebeling, W., Röpke, G.: Ann. Phys. (Leipz.) **36**, 429 (1979)
17. Röpke, G.: Phys. Rev. A **38**(6), 3001 (1988)
18. Morawetz, K., Kremp, D.: Phys. Lett. A **173**, 317 (1993)
19. Esser, A., Röpke, G.: Phys. Rev. E **58**, 2446 (1998)
20. Morawetz, K.: Phys. Rev. E **62**, 6135 (2000). Errata Phys. Rev. E **69**, 029902 (2000)
21. Debye, P., Hückel, E.: Phys. Z. Sowjetunion **15**, 305 (1923)
22. Onsager, L.: Phys. Z. Sowjetunion **8**, 277 (1927)
23. Falkenhagen, H.: Elektrolyte. Hirzel, Leipzig (1953)

24. Falkenhagen, H., Ebeling, W., Kraeft, W.D.: In: Petrucci, S. (ed.) Ionic Interaction, p. 1. Academic Press, San Diego (1971). Chap. 1
25. Kremp, D., Kraeft, D., Ebeling, W.: Ann. Phys. (Leipz.) **18**, 246 (1966)
26. Köhler, H.S., Malfliet, R.: Phys. Rev. C **48**, 1034 (1993)
27. Bozek, P.: Phys. Rev. C **59**, 2619 (1999)
28. Bozek, P.: Eur. Phys. J. A **15**, 325 (2002)
29. Botermans, W., Malfliet, R.: Phys. Rep. **198**(3), 115 (1990)
30. Lipavský, P., Morawetz, K., Špička, V.: Kinetic Equation for Strongly Interacting Dense Fermi Systems. Annales de Physique, vol. 26(1). EDP Sciences, Paris (2001)
31. Bärwinkel, K.: Z. Naturforsch. A **24**, 38 (1969)
32. Ghassib, H.B., Bishop, R.F., Strayer, M.R.: J. Low Temp. Phys. **23**(3–4), 393 (1976)
33. Noguchi, Y., Ishii, S., Ohno, K.: J. Chem. Phys. **125**(11), 114108 (2006)
34. Toulouse, G.: Phys. Rev. B **2**(2), 270 (1970)
35. Gericke, D.O., Kosse, S., Schlanges, M., Bonitz, M.: Phys. Rev. B **59**(16), 10639 (1999)
36. Micnas, R., Pedersen, M.H., Schafroth, S., Schneider, T., Rodríguez-Núñez, J.J., Beck, H.: Phys. Rev. B **52**(22), 16223 (1995)
37. Vagov, A., Schomerus, H., Shanenko, A.: Phys. Rev. B **76**, 214513 (2007)
38. Puff, H.: Näherungsverfahren in der Theorie von Vielteilchensystemen mit direkter Paarwechselwirkung. Preprint 79-1. Zentralinstitut für Elektronenphysik, Berlin (1979)
39. Martin, P.C., Schwinger, J.: Phys. Rev. **115**, 1342 (1959)
40. Fulde, P.: Electron Correlations in Molecules and Solids. Springer Series in Solid-State Sciences. Springer, Berlin (1991)
41. Baym, G., Kadanoff, L.P.: Phys. Rev. **124**(2), 287 (1961)
42. Janis, V.: Phys. Rev. B **64**, 115115 (2001)
43. Janis, V.: J. Phys., Condens. Matter **21**(48), 485501 (2009). doi:10.1088/0953-8984/21/48/485501
44. Prange, R.E.: In: Proc. of Int. Spring School of Physics, Naples. Academic Press, San Diego (1960)
45. Šopík, B., Lipavský, P., Männel, M., Morawetz, K.: Phys. Rev. B. arXiv:0906.3677
46. Beliaev, S.T.: Sov. Phys. JETP **7**, 289 (1958)
47. Gorkov, L.P.: Pis'ma Zh. Eksp. Teor. Fiz. **34**, 735 (1958). Sov. Phys. JETP **7**, 505 (1958)
48. Zimmermann, R., Kilimann, K., Kraeft, W., Kremp, D., Röpke, G.: Phys. Status Solidi (b). Basic Solid State Phys. **90**, 175 (1978)
49. Röpke, G.: Ann. Phys. (Leipz.) **506**, 145 (1994)
50. Röpke, G., Seifert, T., Stolz, H., Zimmermann, R.: Phys. Status Solidi (b). Basic Solid State Phys. **100**, 215 (1980)
51. Röpke, G.: Z. Phys. B **99**, 83 (1995)
52. Kadanoff, L.P., Baym, G.: Quantum Statistical Mechanics. Benjamin, Elmsford (1962)
53. Kraeft, W.D., Kremp, D., Ebeling, W., Röpke, G.: Quantum Statistics of Charged Particle Systems. Akademie Verlag, Berlin (1986)
54. Ward, J.C.: Phys. Rev. **84**(5), 897 (1951)
55. Takahashi, Y.: Nuovo Cimento **VI**, 371 (1957)
56. Velický, B., Kalvová, A., Špička, V.: Phys. Rev. B **77**(4), 041201 (2008)
57. van Leeuwen, R., Dahlen, N.E., Stan, A.: Phys. Rev. B **74**(19), 195105 (2006)